Agriculture, Ecosystems and Environment 219 (2016) 1–13

Contents lists available at ScienceDirect

Agriculture, Ecosystems and Environment

journal homepage: www.elsevier.com/locate/agee

Dynamics of ammonia volatilisation measured by eddy covariance during slurry spreading in north Italy

Rossana Monica Ferrara[a], Marco Carozzi[b,*], Paul Di Tommasi[c], David D. Nelson[d], Gerardo Fratini[e], Teresa Bertolini[f], Vincenzo Magliulo[c], Marco Acutis[g], Gianfranco Rana[a]

[a] Consiglio per la ricerca in agricoltura e l'analisi dell'economia agraria—CREA, Research Unit for Cropping Systems in Dry Environments, via C. Ulpiani 5, 70125 Bari, Italy
[b] INRA, INRA-AgroParisTech, UMR 1402 ECOSYS, Ecologie fonctionnelle et écotoxicologie des agroécosystèmes, 78850 Thiverval-Grignon, France
[c] National Research Council of Italy, Institute for Mediterranean Agriculture and Forest Systems (CNR-ISAFoM), 80056 Ercolano, Italy
[d] Aerodyne Research Inc., Billerica, MA 01821, United States
[e] LI-COR Biosciences GmbH, Siemens Str. 25a, 61352 Bad Homburg, Germany
[f] Euro-Mediterranean Center on Climate Change (CMCC), Via Augusto Imperatore 16, 73100 Lecce, Italy
[g] University of Milan, Department of Agricultural and Environmental Sciences, via G. Celoria 2, 20133 Milan, Italy

ARTICLE INFO

Article history:
Received 16 December 2014
Received in revised form 29 November 2015
Accepted 2 December 2015
Available online 18 December 2015

Keywords:
Emission factors
Incorporation
Closed-path analyser
WPL correction
QC-TILDAS
Inverse dispersion modelling

ABSTRACT

Ammonia (NH_3) emissions have been quantified during slurry spreading in two experimental trials in two intensively managed agricultural fields in northern Italy, during spring 2009 and 2011. NH_3 fluxes have been measured by Eddy covariance (EC) method from the slurry application to the soil incorporation until the end of the emission phenomenon.

The EC system was equipped with a fast sensor for NH_3 concentration measurements based on Tunable Infrared Laser Differential Absorption Spectrometry (QC-TILDAS). NH_3 volatilisation has been monitored in continuous for both experimental trials, confirming the rapidity of the NH_3 losses when slurry is spread to the field. Within 24 h from the application the volatilisation suddenly decreases, stopping after soil incorporation occurred 24 and 30 h from the spreading for the two experimental trials. The maximum NH_3 emission levels were 138.3 and 243.5 $\mu g\, m^{-2}\, s^{-1}$ and the total losses of NH_4-N were 19.4% and 28.5%, determined 7 days after the spreading for the first and the second trial, respectively. EC measurements have been compared to the emissions estimated by a backward Lagrangian stochastic model, resulting consistent for dynamic and quantitative emitted. To explain the differences between the losses in the two experiments, the relationship between emission and meteorological conditions has been investigated. In particular, rain during the 2009 trial caused a significant reduction in emissions, whereas high air temperatures enhanced the emission phenomenon in the 2011 trial. The results shown that for improving nitrogen efficiency, slurry incorporation has to be performed in times closer from spreading than 24 h, under weather conditions which limit NH_3 emissions (such as cloudy with low solar radiation and temperature).

1. Introduction

Ammonia (NH_3) plays an important role in the atmospheric chemistry and is involved in numerous environmental issues related to its emission and deposition (Asman et al., 1998; Galloway et al., 2003). In the 27 member states of the European Union the main source of NH_3 is agriculture where storage and spreading of manure, livestock husbandry and application of synthetic fertilisers are responsible for more than 90% of NH_3 emissions (Reis et al., 2009; EEA, 2011). Since high load of animal breaded, the Po Valley (north Italy) is considered one region in Europe with highest NH_3 emission (Clarisse et al., 2009; Skjøth et al., 2011). Only recently, field scale data of NH_3 emissions have been provided by Carozzi et al., 2012, 2013a,b by means of inverse dispersion modelling based on NH_3 concentration and atmospheric turbulence measurements.

The assessment of NH_3 losses following fertilisation operations is relevant in evaluating the nitrogen (N) balance at field and farm scale and to identify the proper techniques to increase N efficiency. In fact, the agronomic techniques used to supply N fertilisers to the field have direct impacts on the amount of NH_3 released to the environment. The main factors influencing the total amount of NH_3

* Corresponding author. Fax: +33 1 30 81 55 63.
E-mail address: marco.carozzi@gmail.com (M. Carozzi).

http://dx.doi.org/10.1016/j.agee.2015.12.002
0167-8809/

lost from organic and inorganic fertilizers are the concentration of NH_3 in liquid phase and the transfer of NH_3 from this surface to the atmosphere, function of the meteorological conditions, i.e. air temperature, wind speed, solar radiation and field surface roughness (Sommer et al., 1991; Moal et al., 1995; Génermont and Cellier, 1997; Søgaard et al., 2002; Webb et al., 2010). Among these, solar radiation increases surface temperature and air turbulence, increasing the transport of NH_3 to the atmosphere (Sommer and Hutchings, 2001). High temperature increases evaporation, concentrating the total ammoniacal nitrogen (TAN) in the ammoniacal solutions as slurry which, accordingly, encouraging emission because of the lower concentration of NH_3 in the above air layer. The effect of wind speed is strongly related to the emission since wind transports NH_3 upwards, by turbulent transfer, and sideways by advection (Sommer et al., 1991), lowering the NH_3 concentration in the air layer above the solution, stimulating further volatilisation (Génermont and Cellier, 1997). Finally, rainfall and irrigation contribute to dilute the TAN in solutions and enhanced soil infiltration, resulting in an overall reduction of the NH_3 emission rate. Infiltration into the soil can be reduced by the interception of the solutions by the crop canopy or field standing residues, which contribute to extend the NH_3 to atmosphere exchanging surface. In this context, the application method of the fertilisers assumes fundamental importance affecting the NH_3 emission, i.e. application depth, presence or absence of incorporation and infiltration rate into the soil (Huijsmans et al., 2003; Sintermann et al., 2012; Carozzi et al., 2013a,b). However, these factors are combined with the characteristics of the manure, as pH, TAN concentration and dry matter (Van Der Molen et al., 1989; Jarvis and Pain, 1990; Petersen and Andersen, 1996; Génermont and Cellier, 1997; Misselbrook et al., 2000; Sommer et al., 2001).

NH_3 emission quantification is affected by high uncertainties due to challenges in obtaining accurate measurements (von Bobrutzki et al., 2010; Sintermann et al., 2012). This can mainly be attributed to difficulties in measuring fluxes of such reactive compound (Harper, 2005). The hydrophilic nature of NH_3 increases difficulties in its detection (Brodeur et al., 2009), which has to be achieved without modifying the gas-aerosol equilibrium (Mozurkewich, 1993). Furthermore, NH_3 emission by other non-agricultural surrounding sources as transport, wild animals, biomass burning, and agro-industry increases the potential for measurement contamination from the investigated source (Sutton et al., 2000; Dragosits et al., 2010).

Notwithstanding the difficulties described above, in the last decades significant progress has been made in quantifying NH_3 exchange. Sintermann et al. (2012) gives a review of methods available for investigating NH_3 fluxes. At sub-landscape scale, considering that great care must be taken when sampling NH_3 without altering microclimate and soil processes, the use of closed chamber technique is highly questionable (Fehsenfeld, 1995), while open chambers (wind-tunnels) are more appropriate, even if environmental conditions can be modified (Loubet et al., 1999). At field scale, particularly advisable method is the micrometeorological approach for producing long-term trace gas flux time series without altering the microclimate (Denmead, 1983; Kaimal and

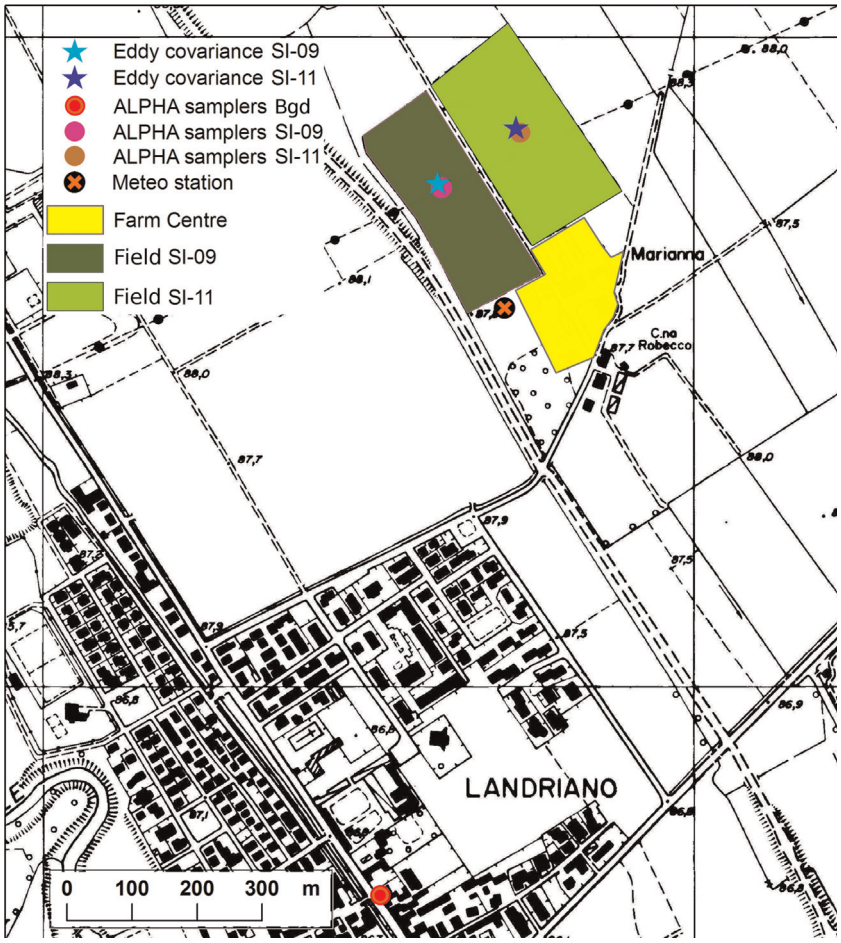

Fig. 1. Site map of experimental fields during the trials in Landriano in 2009 (SI-09) and 2011 (SI-11). The locations of the monitoring stations (Eddy covariance, meteorological and passive ALPHA samplers – see Section 2.2.2) are reported.

Finnigan, 1994). Integrated horizontal flux method is considered a robust approach for spatially limited source area (Denmead, 2008), while the aerodynamic gradient methods or Bowen ratio techniques coupled to wet chemical analysis (Wyers et al., 1993) are the most widely used, as supported by the rich literature (see Sintermann et al. (2012) for a review). Eddy covariance (EC) method is considered the most direct and least error-prone approach for direct flux measurement at the field scale (Denmead, 2008), but it requires a fast gas analyser able to resolve the major part of the turbulent spectrum, which became available only recently. However, only few EC measurements of NH_3 fluxes have been reported in recent papers (Shaw et al., 1998; Famulari et al., 2004; Whitehead et al., 2008; Brodeur et al., 2009; Sintermann et al., 2011; Ferrara et al., 2012). In particular, Ferrara et al. (2012) applied the EC technique with a Quantum Cascade – Tunable Infrared Laser Differential Absorption Spectrometry (QC-TILDAS) for NH_3 concentration measurements, highlighting that proper spectral corrections have to be taken into account in order to compensate the large flux losses of their dataset, which has not been compared to other independent measurements for validating.

In this work the EC method has been used to measure field-scale NH_3 fluxes during two dairy slurry spreading followed by soil incorporation, both performed in the same period and location in the Po Valley. In both cases, high fluxes of NH_3 were expected during the first hours after slurry spreading, with a rapid increasing of NH_3 air concentration. The EC data has been treated and discussed considering the issues related to the application of this method to a sticky gas detected by a closed-path sensor. Moreover, the dynamic of NH_3 volatilisation has been compared with the results obtained by dispersion modelling and discussed in function of the surrounding conditions.

2. Materials and methods

2.1. Experimental sites

The field trials were performed during the springs of 2009 (SI-09) and 2011 (SI-11) in a farm located in Landriano (Po Valley, north Italy, Lat. 45°19′N, Long. 9°16′E, Alt. 88 m a.s.l.). The two experimental fields were situated adjacent to each other and had similar agronomic management (Fig. 1).

SI-09 was carried out from 26th March to 3rd April 2009 in a 3.9 ha field characterised by a loam texture and covered by maize stubbles. The initial soil water content and pH in the 0–20 cm layer were 0.17 $m^3\,m^{-3}$ and 7.1, respectively. The field surface was spread with 87 $m^3\,ha^{-1}$ of dairy slurry on 27th March using splash plate technique (12 m of swath) associated to an umbilical spreading system, a technique which fed slurry to the tractor's distribution system by means of a drag pipe and a pump connected to the slurry storage tank. The application started at 8:00 a.m., from the west edge to the opposite one, along the longer side of the field. After 24 h from the beginning of the spreading, the slurry was incorporated by means of a combined disc harrower working at a depth of 25 cm. The operations of spreading and harrowing lasted 7 and 1.5 h, respectively. The total ammoniacal nitrogen (TAN) applied was 95 kg NH_4-N ha^{-1}.

The SI-11 was performed from 6th to 13th April 2011 in a 4.3 ha loam texture soil covered by sparse 10 cm tall *Lolium multiflorum* Lam. The initial soil water content and pH in the 0–10 cm layer were 0.21 $m^3\,m^{-3}$ and 6.4, respectively. Dairy slurry was applied on 7th April at 8:30, at a rate of 75 $m^3\,ha^{-1}$ starting from the east edge of the field and proceeding towards the opposite side, following the longer side of the field. The spreading and incorporation techniques were similar to SI-09; the spreading lasted 5 h, while the incorporation started 30 h after the beginning of the slurry application and lasted 2 h. The TAN applied was 109 kg NH_4-N ha^{-1}.

Table 1
Main features of the slurries applied during the trials in Landriano 2009 (SI-09) and 2011 (SI-11). TAN is total ammoniacal nitrogen and TKN is total Kjeldahl nitrogen, the sum of organic nitrogen, NH_3 and ammonium. Values refer to fresh weight. Standard error is in the brackets.

	Dry matter ($g\,kg^{-1}$)	pH (–)	TAN ($g\,kg^{-1}$)	TKN ($g\,kg^{-1}$)
SI-09	44 (0.09)	8.0 (0.07)	1.09 (0.004)	2.16 (0.02)
SI-11	55 (0.06)	7.8 (0.10)	1.45 (0.091)	2.97 (0.16)

The characteristics of the slurries used in the field trials are summarised in Table 1. The spreading method was consistent with the agronomic practices of the local farmers.

Furthermore, meteorological variables were measured with a standard station (Lastem, Milan, IT) working at hourly time step, respectively at 180 and 250 m away from the centre of the SI-09 and SI-11 fields (see Fig. 1). Air temperature, relative humidity (*RH*), global solar radiation and precipitation were measured at 1.8 m above ground.

2.2. NH_3 concentration measurements

2.2.1. The QC-TILDAS for fast NH_3 measurements

The fast NH_3 concentration analyser employed during the trials is manufactured by Aerodyne Research Inc. (ARI, Billerica, Massachusetts, USA) and is described in detail in Nelson et al. (2002) and Ferrara et al. (2012). This device consists of a pulsed QC laser (Alpes Lasers, Neuchâtel, Switzerland), an optical system, an astigmatic Herriott type multiple pass absorption cell (optical absorption path length 76 m, volume 0.5 L), a thermo-electrically cooled photovoltaic detectors (Vigo Systems, Poland) and a computer-controlled system that incorporates the electronics for driving the QC laser along with signal generation and data acquisition. The QC-TILDAS determines NH_3 mole fractions (mole NH_3 per mole of wet air) by monitoring the molecule's absorption of radiation at 967 cm^{-1}, using the ARI's software package TDLWintel. In order to test the performance of the QC-TILDAS in detecting NH_3 concentrations, during the field measurement an automatic procedure was performed every 6 h by using a certified NH_3 tank (1 ppm of NH_3). These data were used to identify a multiplier, equal to 3.0, which has to be adopted to reproduce the right atmospheric NH_3 value. In fact, laboratory tests demonstrated that the analyser underestimates NH_3 values, so a post-processing calibration has to be done introducing a multiplier to reproduce the correct NH_3 concentration values (Ferrara et al., 2012). Moreover, in order to understand the origin of the underestimation of NH_3, further laboratory tests using a standard of ethylene (C_2H_4) were performed. This compound has an absorption line in the region scanned by the instrument (Fig. 2), but it has not the sticky nature as NH_3. Thus, the use of C_2H_4 gives the chance to test whether the NH_3 underestimation by the QC-TILDAS is explainable in term of the spectroscopic features of the QC laser source or rather, if it is due to the sample passage in the inlet line. Actually, the tests showed that C_2H_4 and NH_3 presented similar calibration factors, whose origin is thus to be attributed to the spectral width of the pulsed laser. It is worth noting that continuous-wave quantum cascade lasers are now available with sharp spectral line width which allows calibration factors very close to unity.

During both trials, air samples were collected through a sampling tube heated at around 30 °C (Whitehead et al., 2008). The tube was 1.80 and 1.45 m long for SI-09 and SI-11, respectively, with 9.6 mm of inner diameter and made in inert paraformaldehyde (PFA). The sampling line was designed so as to avoid using particulate filters and any interference they may cause.

In proximity of the analyser the flow was restricted with a small glass orifice and partially deviated with a sharp 90° turn to the

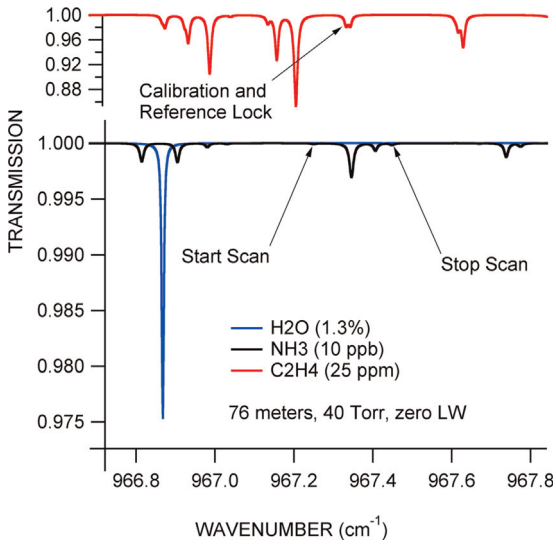

Fig. 2. Scan regions of the employed QCL source and peak positions of the ethylene (C_2H_4), ammonia (NH_3) and water (H_2O). Multipass cell characteristics of the test are reported, optical absorption path length 76 m, internal pressure 40 Torr and zero laser width.

multi-pass cell using a tee junction and two vacuum pumps, the first downstream the cell (VARIAN TriScroll 600 Series) and the second at the other side of the tee junction (VARIAN, mod SH110). This setup avoids fast contamination of cell optics as particulate tend to flow strait at the tee junction. The orifice sensibly reduced the air flow at the inlet, about 3 L/min for both years whereas the flow rates towards the analyser were about 2.4 L/minute for SI-09 and 2.3 L/min for SI-11. The tube connecting the tee junction to the cell was 15 and 30 cm long and the pressure inside approached the cell pressure, 4.7 kPa in SI-9 and 1.4 kPa in SI-11, resulting in a cell response time of 0.5 and 0.15 s, respectively. In fact, the multi-pass cell pressure values have to balance between minimising line broadening and adsorption effects, maximising time response and achieving good sensitivity (Warland et al., 2001). In the other hand, the orifice in the inlet line generates a laminar flow regime in the sample tube and this could explain the large spectral correction at high frequencies as reported also in Ferrara et al. (2012).

To ensure a proper functioning of the whole system, the QC-TILDAS box was maintained at 20 °C by means of an air-conditioning system in order to avoid overheating and instrumental drifts due to air temperature daily trends.

2.2.2. Passive diffusion samplers for long term concentration measurements

During the field trials, NH_3 concentrations were also measured by means of a passive and time averaged approach, based on ALPHA samplers (Adapted Low-cost Passive High Absorption, Tang et al., 2001; Sutton et al., 2001). The operating principle of these samplers is based on the capture of gaseous NH_3 on a filter paper covered by citric acid (13% m/v). During the trials, a set of three samplers was placed in the field centre to measure the slurry emissions, while background concentration was assessed by another set of three samplers placed 1200 m far upwind from the fertilised area any known NH_3 source (see Fig. 1). A background sampling point was placed 2.3 km south-east in SI-09, to further assess the environmental background ammonia. The field samplers were exposed at the same height of the QC-TILDAS inlet for a time interval no longer than 12 h, reduced up to 2 h during the day of the slurry application and, only for SI-11, the day after spreading. After the exposure the filters were extracted in 3 ml of deionised water and the NH_4-N content determined by the indophenol blue colorimetric method and spectrometry (FOSS, FIAstar 5000 system, Denmark).

2.3. NH_3 fluxes

2.3.1. Eddy covariance method

The vertical flux of NH_3 is given in terms of the covariance between instantaneous vertical wind speed and NH_3 concentration, with an average time interval of 30 min in our case. The effects of changing air density must be considered by including the so-called WPL terms (Webb et al., 1980). Conventionally this aspect has been thoroughly discussed for open-path EC systems (Baldocchi, 2003), while recently Ibrom et al. (2007) systematised the topic also for closed-path applications.

The relative importance of WPL terms depends on the background concentration of the gas and the magnitude of the flux (Denmead, 1983; Liebethal and Foken, 2003), typically being negligible for trace gas with small background concentration and large fluxes, such as in the present case with NH_3 by a strong source like a slurry spreading. However, the correct consideration of density effects is still controversial when closed-path gas measurements are available as mole fractions and parallel measurements of water vapour in the instrument absorption cell are not available (Hiller et al., 2012).

The EC stations were located in the centre of each field, orthogonally at 78 m and 93 m far from the longer edges of the field, for SI-09 and SI-11, respectively. The systems were both equipped with a three-dimensional sonic anemometer (Gill-R2, Gill Instruments Ltd, UK) and the QC-TILDAS used to measure NH_3 concentration. The inlet tube was placed close enough to the measuring volume of the sonic anemometer and at 1.45 m and 1.25 m above ground for SI-09 and SI-11, respectively. The analogue signals from the QC-TILDAS were transmitted to the sonic anemometer, which acquired at 20.8 Hz: the digitised signals from the QC-TILDAS were synchronised and combined with the wind velocity data and then acquired via EddySoft software (Kolle and Rebmann, 2007), while half-hourly NH_3 fluxes were computed offline by using EddyPro® 4.2 (www.licor.com/eddypro). Double-rotations were applied to compensate any tilting of the sonic anemometer (Wilczak et al., 2001) and the angle-of-attack corrections, after Nakai et al. (2006), have been applied to compensate flow distortions: its value ranged between 13 and 15% for the two trials. No detrending was used and turbulent fluctuations where estimated using blocks averaging. Since a non-constant time lag between sonic and NH_3 concentration data has been observed, in order to maximise the covariance, the time lag for each averaging period has been taken into account. In fact, for both the trials the determination of the time lag was defined during the high emission periods (e.g. the initial fluxes after the spreading), becoming noisy during the subsequent low flux events. The use of a fixed time lag leads to a general flux reduction of about 15%. Applying this value to the periods characterised by noisy time lags (i.e. the end of the emission phenomenon), a reduction of the emission less than 0.01% occurs, contributing for 0.3 and 1% of total emission for SI-9 and SI-11, respectively.

To estimate the portion of the upwind source contributing to the measured fluxes at the measurements heights, a footprint analysis following Kormann and Meixner (2001), was performed. This analysis combines Eddy covariance measurement data and land use information as detailed in Neftel et al. (2008).

2.3.2. Quality check and data screening

High frequency NH_3 data were visually analysed for spike detection finding reasonable values up to 4000 ppm. Flagged data were excluded and replaced by linear interpolation between adjacent points. In order to examine the site setup and assess the

overall validity of the fluxes, the flux-variance similarity was analysed for vertical wind velocity and sonic temperature variances (Kaimal and Finnigan, 1994). This similarity means that the ratio from the standard deviation of the turbulent parameter and its turbulent flux has to be nearly constant or a function of the atmospheric stability. Here we used the similarity equation given for unstable and near neutral conditions adopted in Aubinet et al. (2012) to predict theoretical behaviour:

$$\frac{\sigma_w}{u_*} = 1.25\left(1 + 3|\frac{z}{L}|\right)^{1/3}$$

$$\frac{\sigma_T}{T_*} = 2\left(1 + 9.5|\frac{z}{L}|\right)^{-1/3}$$

where σ_w and σ_T are the standard deviation of vertical wind component and sonic temperature, respectively, u_* is the friction velocity, z is the height above the zero plane displacement, L is the Obukhov stability length and $T_* = \overline{w'T'}/u_*$. The results, expressed in terms of deviation from the theoretical prediction, are reported in Table 2. Since the scalar fluxes are affected by large relative errors, the final dataset (15 and 39% of data for SI-09 and SI-11, respectively) does not contain periods of atmospheric stability and near neutral conditions. On the other hands, this dataset contains data for which the sensible heat flux density is more then 20 W m^{-2}. Following Foken and Wichura (1996), data are considered to have a good quality when the deviation from the calculated value does not exceed 20–30%. The large agreement between the measured values and the theoretical prediction suggests that the measurements performed have to be considered valid and representative, despite the low measuring height and the restricted fetch.

In order to discard data obtained when the assumptions in turbulent flux calculation fails, all flux data were sorted into 3 quality classes following Mauder and Foken (2004): 0 for best quality fluxes, 1 for fluxes suitable for general analysis and 2 for fluxes that should not be used. This widely adopted procedure uses a combination of partial flags calculated as a result of the integral turbulence test, based on the flux variance similarity, and the stationarity test. This latter verifies the steady state of fluxes within the averaging period (Foken and Wichura, 1996). The 30% of available data for both experiments was assigned to class 2 and consequently discarded and excluded from the subsequent analysis (Table 2). A number of studies (e.g. Mauder et al., 2013) demonstrated the efficiency of this flagging system to eliminate unrealistic data and minimise stochastic errors within an average of 20–30% for 0–1 class data.

2.3.3. Flux correction

Flux losses due to spectral attenuations are inevitable in any EC system and more so in closed-path systems equipped with an intake tube (Leuning and Moncrieff, 1990). Nowadays, a variety of methods can be chosen to compensate such losses by means of frequency response correction factors (e.g. Eugster and Senn, 1995; Massman, 2000; Ibrom et al., 2007; Fratini et al., 2012). The magnitude of these losses can be as high as 40% of the actual fluxes, as reported by Ferrara et al. (2012) for NH_3 fluxes from urea measured with the same equipment. In the present case, following Moncrieff et al. (1997), the spectral correction of the measured NH_3 fluxes has been applied by using the EddyPro® package, resulting in a mean correction around 49 and 45% for SI-09 and SI-11, respectively. In particular, to correct the measured fluxes the approaches detailed in Ferrara et al. (2012) were applied, finding that the spectral theoretical transfer functions (TF) implemented in the EddyPro® package gave results comparable to the in situ methods (Massman and Clement, 2004). The theoretical TF method is purely analytic and models all major sources of flux attenuation due to the instrumental setup by means of a mathematical formulation. This method is suggested for open path EC systems or for closed path systems if the sampling line is short and heated, such is this case. In fact, it is to be noted that in the current application, effects of relative humidity were minimised by heating the sampling line so as to decrease relative humidity of the sampled air and avoid strong *RH*-dependent attenuations. In the method of Moncrieff et al. (1997) the first step is to estimate true cospectra using analytical cospectra formulations, according to Eqs. (12)–(18) in that paper. Afterwards, a low-pass transfer function (LPTF), which depends on the EC system characteristics, is specified by the superimposition of a set of TFs, describing individual sources of high-frequency (HF) losses. The mathematical formulation for the individual TFs is detailed in the Appendix A in Moncrieff et al. (1997). In particular, Moore (1986) developed theoretical TFs for compensating the attenuation due to the dynamic frequency response of the sensors, the scalar path averaging, the sensor separation (0.30 cm in our case) and the sensor response mismatch, while Moncrieff et al. (1997) gave a complete description of TFs of EC systems with closed-path analysers. For the EC system used in both the experiments, a non-negligible effect on the HF losses is given by the tube sampling. In fact, the damping effect produced by the tube was modelled following Lenschow and Raupach, (1991) for describing the attenuation of the fluctuation of concentrations down to the sampling tube, in which the flow regime was laminar. The needed parameters for this TF are the tube radius, 0.95504 cm, the molecular diffusivity of the scalar, around 0.2 cm^2 s^{-1} for NH_3 (Massman, 1998), the tube's length and the flow rate. Finally, flux attenuation in the HF end is estimated by applying the calculated LPTF to the estimated true flux co-spectrum.

Fig. 3 shows a typical NH_3 flux co-spectrum over the natural frequency and visualises its attenuation by comparison with the simultaneous sensible heat co-spectrum. NH_3 cut-off frequencies have been evaluated using Aubinet et al. (2000) and were about 0.34 and 0.38 Hz for SI-09 and SI-11, respectively, values which can be found in literature when close path system are employed (Yasuda and Watanabe, 2001; Eugster et al., 2007; Ibrom et al., 2007; Bariteau et al., 2010). In general when EC technique is used, the cospectra usually present erratic variability deviations in the low to mid frequencies, when compared with those described by Monin–Obukhov similarity theory (Foken et al., 2012). Furthermore, in this case of NH_3 flux measurements during slurry spreading, the temporal variation in NH_3 concentration showed sudden and episodic bursts of higher values, such as one expects from a process that is not perfectly continuous, but event-driven, exactly as found By Eugster and Plüss (2010) for methane fluxes (see their Fig. 11a). This implies that the conventional cross-correlation procedure, usually used to define the actual time lag between vertical wind speed data and the NH_3 concentration, often does not lead to clearly see the time lag as is normally the

Table 2
Quality tests results for NH_3 flux data (classes 0–2) following Mauder and Foken (2004). Flux variance similarity results for vertical wind (σ_w/u_*) and for sonic temperature (σ_T/T_*) following Aubinet et al. (2012). The number and percentage of data belonging to each quality class and for the 3 classes of deviation from calculated values are reported.

		Quality class			Test σ_w/u_*			Test σ_T/T_*		
		0	1	2	<20%	20/50%	≥50%	<20%	20/50%	≥50%
SI-09	# data	48	98	64	25	6	1	19	9	4
	%	23	47	30	78	19	3	59	28	13
SI-11	# data	71	121	83	98	7	2	74	20	13
	%	26	44	30	92	7	2	69	19	12

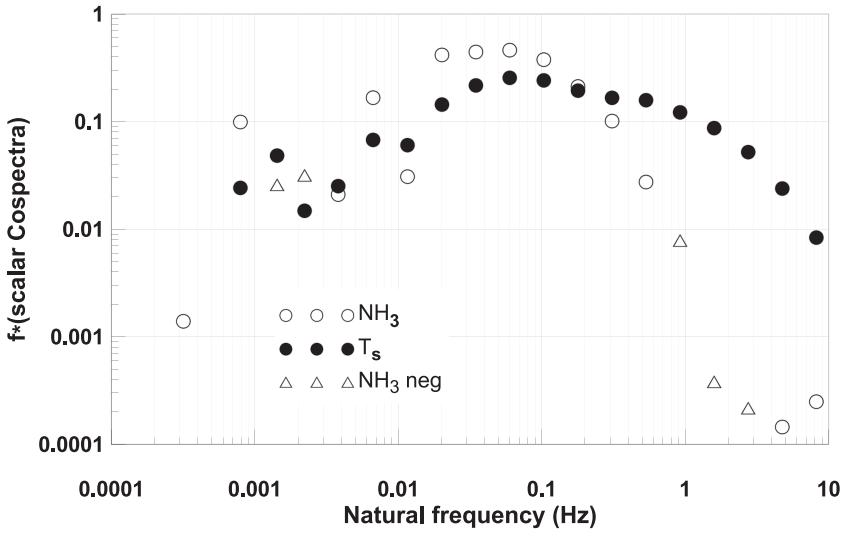

Fig. 3. Normalised averaged co-spectra (ratio of co-spectra over covariance) of NH_3 and sensible heat fluxes (T_s) over a 1.5 h period (day 27 March 2009, from 12:00 a.m. to 1:30 p.m., with $U = 1.4\,m\,s^{-1}$ and $z/L = -0.3$). The negative values of NH_3 co-spectrum (NH_3 neg) have been inverted to be represented on the logarithmic scale.

case with other scalars. Thus, the definition of a temporal window for finding the peak of correlation has to be strongly narrowed even in case where episodic plumes of NH_3 lead to a considerable cross-correlations, with respect to the time delay between vertical wind speed data and the scalar concentration. This episodic nature of NH_3 effluxes in our experiments also explains the less smooth cospectra of the ammonia (our Fig. 3) than what is usually experienced for other scalars cospectra. Moreover, at higher frequencies, NH_3 co-spectrum is also noisier and its values sometimes being negative. These negative values have been shown as absolute values, as suggested by Mammarella et al. (2010).

While the air density fluctuations induced by temperature are efficiently dumped through the heated sampling line to the absorption cell, the concentration measurements in terms of mole fraction require the consideration of density fluctuations due to water vapour fluctuations—the WPL term discussed above. In this regards, for the instruments that are not able to measure fast H_2O concentrations, several approaches have been reported in the literature (e.g., Smeets et al., 2009; Detto et al., 2011; Hiller et al., 2012). If fast H_2O measurements are performed with a parallel instrument running beside the NH_3 analyser inlet, H_2O fluctuations could be used in the WPL term, as in Detto et al., (2011). In our application fast H_2O measurements from an open-path LI-7500 (LI-COR Biosciences Inc., Lincoln, NE, USA) were used finding a relative correction $\leq$1%. Therefore, this minimal contribution of the WPL term could be safely neglected also because it refers to open air H_2O fluctuations measured with an open path infrared gas analyser, whereas the H_2O fluctuations in the NH_3 analyser cell are dumped trough the sampling tube, consequently lowering the WPL term contribution.

About the cross-sensitivity to water vapour, as reported by Neftel et al. (2010), even if all infrared gas analysers may show some response to the gas-matrix, especially to water vapour, the effect is expected to be less significant for pulsed QCL since their lower spectral resolution tends to make them less sensitive to spectral details. Therefore, for this study, we did not take into account the cross-sensitivity to H_2O: although it may be possible to simultaneously measure NH_3 and H_2O (setting the laser to use the nearby water line shown in Fig. 2), the wider scan would degrade the NH_3 measurement sensitivity, making it harder to measure low NH_3 fluxes.

2.3.4. Dispersion modelling

The backward Lagrangian stochastic (bLS) model WindTrax (Thunder Beach Scientific, Halifax, Canada; version 2.0.8.8) detailed in Flesch et al. (2004) has been employed to infer NH_3 emission from the concentration measurements. The model determinates the concentration to emission ratio as the number of the interactions between the source area and the number of trajectories (50,000 for every integration time) upwind from the concentration measuring points. Data required are the turbulence parameters as u_*,L, wind direction and the roughness length measured by the sonic anemometer at integration times of 30 min,

Table 3
Main statistics (mean, maximum, minimum and cumulated) of weather variables, friction velocity, u^*, and stability parameter, z/L, during the trials in Landriano 2009 (SI-09) and 2011 (SI-11). *RH* and *U* are relative humidity and wind speed, respectively.

		Rain (mm)	Temperature (°C)	RH (%)	U ($m\,s^{-1}$)	Global solar radiation ($W\,m^{-2}$)	u_* ($m\,s^{-1}$)	z/L (–)
SI-09	Mean		11.2	94.5	1.5	85	0.14	0.045
	Max		19.4	100	5.6	630	0.41	2.7
	Min		3.1	71.5	0	0	0.02	−1.48
	Cumulated	55						
SI-11	Mean		18.5	86	1.3	222	0.15	−0.066
	Max		32	97	3.4	823	0.41	18.1
	Min		7.5	16	0	0	0.01	−62.3
	Cumulated	0.0						

NH_3 concentrations obtained by the QC-TILDAS, the background concentrations measured by ALPHA samplers and the geometry of the source area (GPS recorded).

The source is considered as homogeneous exchanging surface, no atmospheric reaction of the gas is accounted and, for these simulations, roughness length is fixed (0.018 and 0.04 m for SI-09 and SI-11, respectively). The turbulence parameters were also filtered in order to remove the condition when the Monin–Obukhov similarity theory is no longer considered valid (Hensen et al., 2009; Loubet et al., 2009; Flesch et al., 2014). The imposed thresholds were $|L| > 2$ m and $u_* > 0.05$ m s^{-1}. Moreover, the threshold for u_* was also evaluated from 0.05 to 0.16 m s^{-1} in order to evaluate the applicability of the Monin–Obukhov similarity theory and the emission rate.

3. Results and discussion

3.1. Micrometeorological data

Table 3 present the statistics of hourly weather data and micrometeorological data (u_*, and the atmosphere stability parameter (z/L)) detected during the two trials. During SI-09, the main wind direction was east (Fig. 4a) and an important rain event of 55 mm occurred within the 24 h after the incorporation. During SI-11, the prevailing wind direction was west (see Fig. 4b), no rain occurred and the air temperature was higher than during 2009, even if the meteorological conditions during the two trials were within the seasonal averages (period 1988–2011). Fig. 5 reports the trends of z/L, u_* and wind speed during both trials. The stability parameter displayed general nocturnal stability peaks (positive) and negative values during daily atmospheric instability, especially during SI-11. The u_* showed a typical daily maximum with minimum at night, following the course of the wind speed. However, during the rain event occurred in SI-09 starting from 28th March night, the values of u_* were almost constant and low (see Fig. 5a).

3.2. Footprint

The analysis of the footprint is summarised in Table 4. During SI-09, 89 and 87% of fluxes come from inside the field during daytime and night time respectively, while during SI-11 the 96 and 94% of fluxes come from inside the field during daytime and night time, respectively. The value of the length reached by the footprint during the night time is due to the atmospheric condition characterised by high stability (see Fig. 5), where the vertical concentration gradient of the scalar are enhanced to very small diffusivity and the extension of the atmospheric boundary layer increases. The source area resulted included in the field treated by slurry in both the trials, despite the presence of a tree lined in the sides north and west in the field SI-09, north and east in SI-11. The footprint mean peak positions were at 12 and 7 m from the mast, for SI-09 and SI-11, respectively. Finally, the maximum of the footprint peak during the trial SI-09 was smaller than SI-11 during both the daytime (40 m against 61 m) and night time (76 m against 164 m), mainly due to the higher atmospheric stability occurred of SI-11.

3.3. NH_3 concentrations and fluxes

Fig. 6 reports the NH_3 concentrations measured by the ALPHA passive samplers and by the QC-TILDAS, averaged over the exposure time of the passive samplers. Obviously, the different time resolution of the two systems prevents the direct comparison between the maximum NH_3 concentrations recorded in the field, even if all the other statistics computed on the whole experimental period are comparable. Moreover, the NH_3 concentration trends detected by the two devices result similar as shown in Fig. 6a and b, confirming the validity of the collected data: root mean square error (RMSE) 114.3 and 102.5 μg NH_3 m^{-3}, coefficient of determination (R^2) 0.89 and 0.9, slope (x: ALPHA; y: QC-TILDAS) 1.21 and 0.95, coefficient of residual mass (CRM) −0.04 and −0.06, for SI-09 and SI-11, respectively. In SI-09 it can be noticed a clear difference between the concentrations of the QC-TILDAS and ALPHA, especially during the night after the spreading (28th March 2009). This is probably due to an obstacle between the natural diffusion of the gas and the surface in contact with the atmosphere of the passive samplers, potentially caused by surrounding environmental conditions: high humidity (97.7% in this period of integration), low temperature (11.7 °C) and the scarceness of wind (0.88 m s^{-1}).

The hourly NH_3 concentration values (with standard deviations) and fluxes measured during the two trials are reported in Fig. 7a–d. In Fig. 7 the air and soil surface temperatures, *RH*, global solar radiation and the rainfall are also reported. The comparison between the two trials in terms of NH_3 concentration shows different dynamics, even if the spreading techniques were similar in the two years. In fact, firstly, the concentration values detected by the QC-TILDAS during the trial SI-11 are higher than the ones recorded during SI-09 (Fig. 7a and b). Secondly, during SI-09, the peak value of NH_3 concentration was reached 1.5 h after the end of slurry spreading, starting to smoothly increase 2 h after the start of the spreading (Fig. 7a). During SI-11 the maximum values were reached during the spreading (Fig. 7b) and the rising of the concentration was sudden and rapid. Moreover, during SI-09, after the first main peak, NH_3 concentration showed other peaks occurring during the early night, decreasing in the following day. In this case it is clear that the soil tillage due to the incorporation of

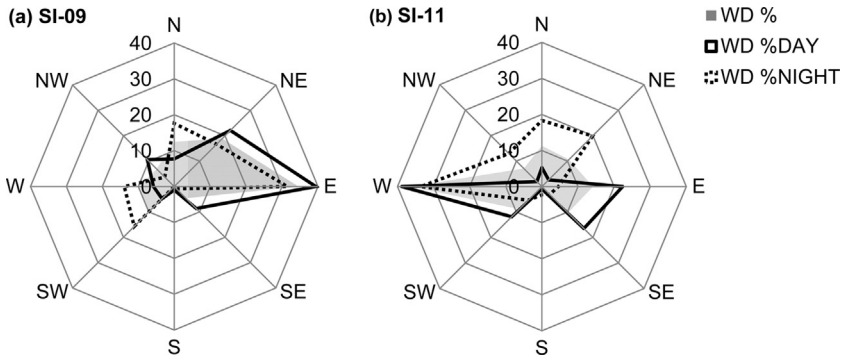

Fig. 4. Main and day–night wind direction (WD) during the trials: (a) Landriano 2009 (SI-09) and (b) 2011 (SI-11).

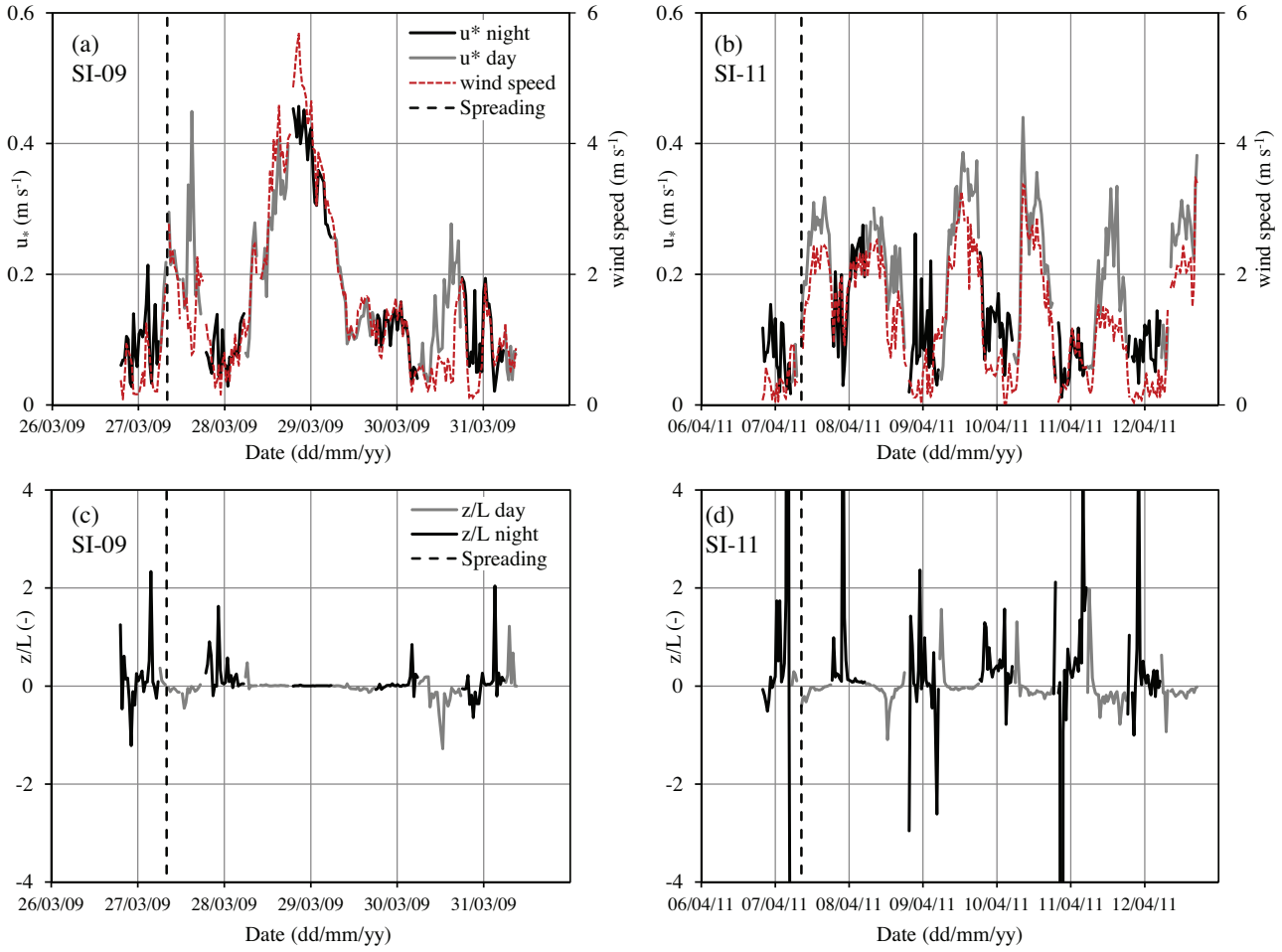

Fig. 5. Trials Landriano 2009 (SI-09) and Landriano 2011 (SI-11): (a and b) wind speed and friction velocity (u_*); (c and d) stability parameter z/L. The daytime and night time trends are reported.

Table 4
Statistic of footprint during daytime and night time in Landriano 2009 (SI-09) and 2011 (SI-11) following Neftel et al. (2008). Distance is named the distance from the sensor to the ellipse that approximate the contour where the crosswind-integrated footprint function reaches 1% of its maximum value; Length is the length of the footprint, difference between the value where the footprint function drops below 1% of its maximum value and the Distance; Width is the width of the ellipse at the centre of length. Field is the percentage of the field in the footprint.

		Daytime				Night time			
		Distance (m)	Length (m)	Width (m)	Field (%)	Distance (m)	Length (m)	Width (m)	Field (%)
SI-09	Mean	1.9	101	54	89	1.9	112	66	87
	Max	7.9	591	228	98	14.2	1165	904	98
SI-11	Mean	1.4	68	48	96	1.0	69	58	94
	Max	9.4	738	498	98	6.3	523	956	99

the slurry dropped the concentration of NH_3 in the air above the soil. The effectiveness of the incorporation in reducing NH_3 emission, more evident during SI-09 than in SI-11, occurred also at high levels of u_*, with a potential transport for the investigated gas (see Fig. 3). Furthermore, the rain event occurred towards the end of the day of the incorporation, reduced even more the emissions. The trends of NH_3 concentration observed during SI-11 (Fig. 7b) showed two close peaks, caused by a break of 2 h during the slurry spreading due to a tractor fault. Afterwards, the concentration values showed a reduction, with a further decreasing after the slurry incorporation. After the tillage, the NH_3 concentration remained low and near to the reference background value, except for small peaks in the early evening of the same day.

During both the trials, the NH_3 fluxes estimated by EC (see Fig. 7c and d) showed similar trends such as the concentrations dynamics. NH_3 fluxes were close to zero before the beginning of the slurry spreading, followed by a sudden increasing in NH_3 volatilisation during the warmer hours of the same day. The maximum flux during SI-09 was reached just after the end of slurry distribution, 138.3 $\mu g\,m^{-2}\,s^{-1}$ at 4 p.m., while during SI-11 a double peak pattern of 243.5 and 156.1 $\mu g\,m^{-2}\,s^{-1}$ at 11:30 a.m. and 4:00 p.m., respectively, was observed. This last behaviour is

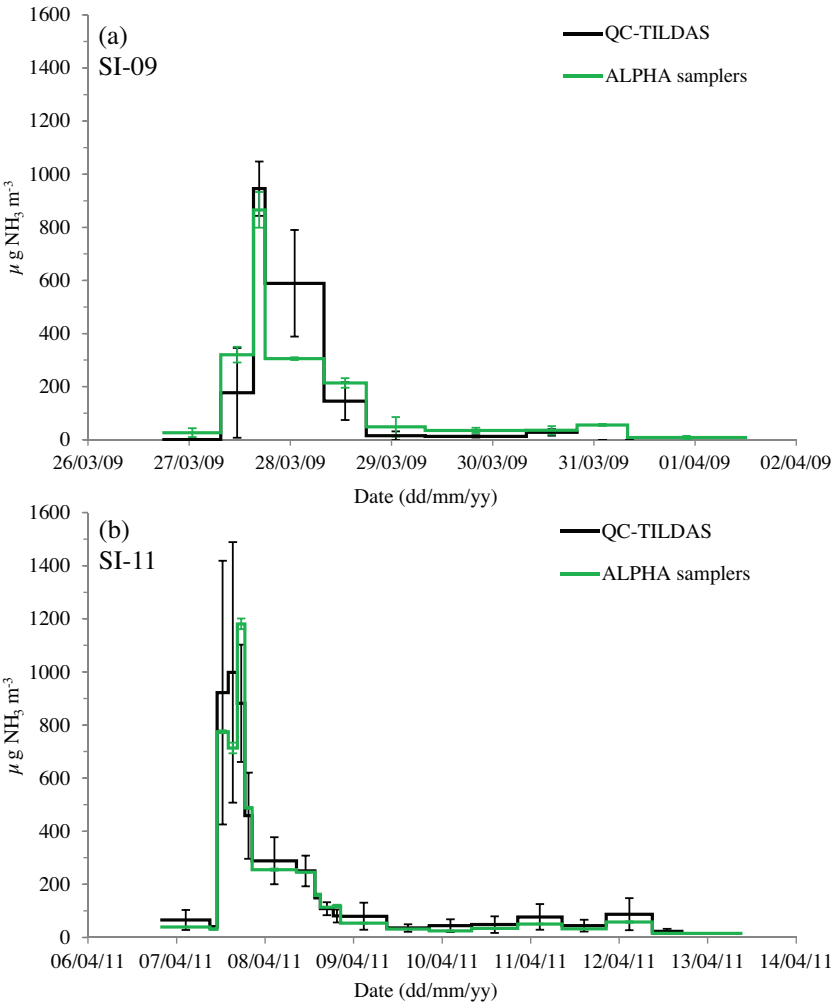

Fig. 6. NH_3 concentration measured by the fast analyser (QC-TILDAS) and the passive samplers (ALPHA) at the time resolution of the ALPHA samplers during: (a) Landriano 2009 (SI-09) and (b) Landriano 2011 (SI-11).

linked to the breaking in the spreading operation, as above mentioned. In both cases, the NH_3 fluxes suddenly decreased during the evening with a small upturn in NH_3 emission at the beginning of the day after of 28.3 and 18.5 $\mu g\,m^{-2}\,s^{-1}$ for SI-09 and SI-11, respectively. The slurry incorporation dropped the values of NH_3 emission and, until the end of the measuring period, no significant other NH_3 fluxes were detected.

The difference in magnitude of the NH_3 fluxes during the two trials could be explained in terms of difference of weather conditions. In particular, the higher air temperatures of SI-11 than SI-09 (see Fig. 7c and d and Tables 3 and 4) seem to be identified as one of the drivers of the volatilisation phenomenon (Sommer et al., 1991), which was stopped by rainfall events and the decreasing of air temperature occurred during SI-09. As reported by Sommer and Hutchings (2001), numerous studies have found positive relationships between NH_3 emission from surface-applied manure and incident solar radiation or air temperature. In our case, during SI-09 the weather was cloudy with low solar radiation, while the trial SI-11 was carried out under sunny conditions: the relationship between emission and air temperature can be considered a reflection of the warming effect of solar radiation.

However, even if the incorporation occurred in different times and the amount of NH_3 losses was different during the two trials, the time dynamic was very similar. In particular, looking the normalised cumulated NH_3 losses (Fig. 8), it is clear that in both the trials, even if in SI-11 the soil incorporation occurred after 30 h from the spreading, the significant losses occurred within the first 24 h from the slurry spreading, stopping definitively after the slurry incorporations. The total amount of NH_3 volatilised on the first 24 h was 16.8 and 29.85 kg N ha^{-1} for SI-09 and SI-11, respectively, corresponding to the 91.3 and 89.1% of the total TAN loss by volatilisation. The NH_3 EFs for the two field trails were 19.4% and 28.5% of the TAN applied for SI-09 and SI-11, respectively. Removing periods in which Eddy fluxes can be considered as unreliable by adding a range of lower threshold of friction velocity ($u_* \geq 0.05$ to 0.16 $m\,s^{-1}$) and filling the gaps by using linear interpolation between available data points, the resulting emissions varying in a range from 19.4 to 26.6% for SI-09 and from 28.5 to 29.7% for SI-11. One of the reason of the bigger range achieved in SI-09 is due to the stable conditions occurred during the end of the spreading and the day after, mainly for the rain event, and the linear interpolation procedure that has filled up to 44% of the data for the higher value of the u_* threshold.

The results obtained in these field trials are comparable with previous studies carried out in similar conditions (see the review of Sintermann et al., 2012). Considering NH_3 fluxes measured during slurry surface spreading, at field scale and on arable land, SI-09 reports volatilisation in the same order of magnitude compared to those reported by Sintermann et al. (2011) using EC: flux maximum peak of 150 $\mu g\,m^{-2}\,s^{-1}$ and 15.7% of volatilised NH_3.

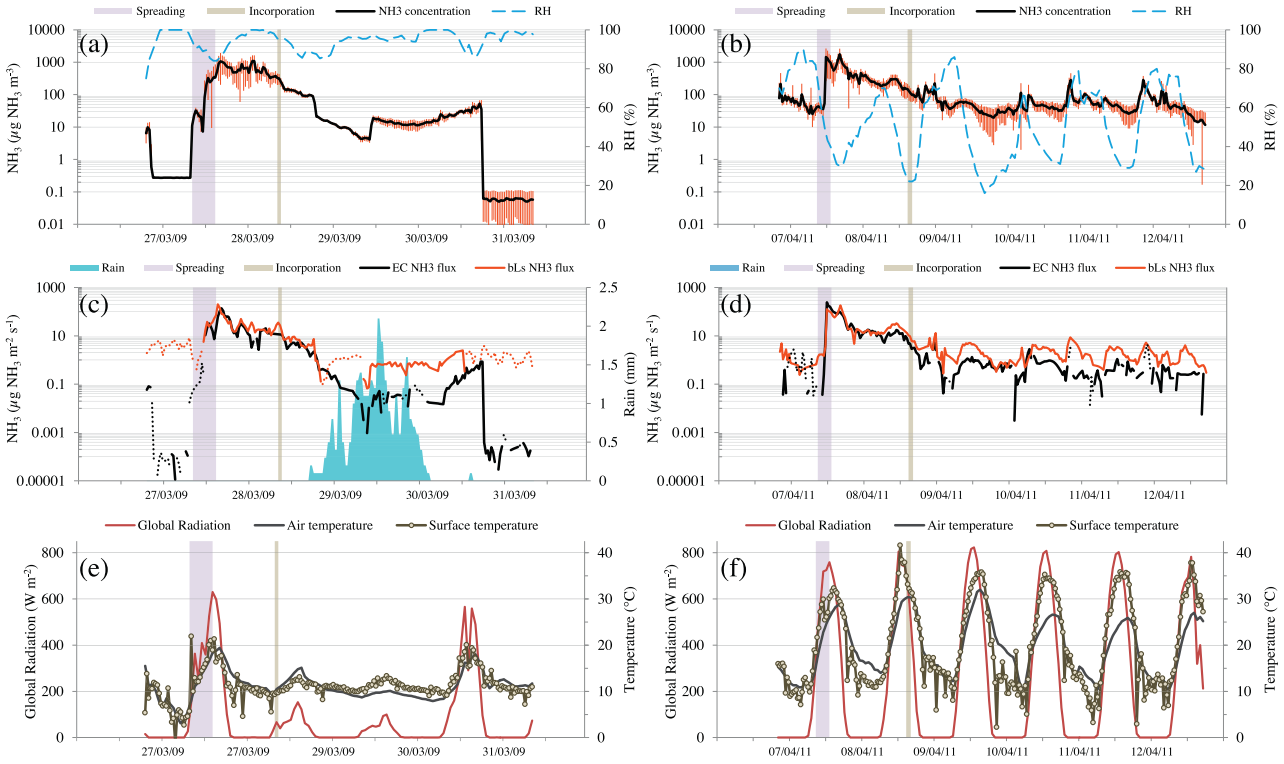

Fig. 7. Trials Landriano 2009 (SI-09) and Landriano 2011 (SI-11): (a and b) NH_3 concentration in logarithmic scale with the standard deviation measured by the QC-TILDAS; (c and d) NH_3 fluxes estimated by using the Eddy covariance system and the backward Lagrangian stochastic model (bLS), in logarithmic scale. Dotted line represent the negative values of NH_3 flux, inverted to be represented on the logarithmic scale. The rainfall, the relative humidity, the soil surface and air temperature, the times of slurry spreading and incorporation are reported too.

NH_3 emissions by the inverse dispersion modelling provide comparable results in terms of dynamic and total emissions with EC system, as shown in Fig. 7c and d, that report the trends of the bLS source estimation alongside the EC flux measurement for the two filed experiments. In Fig. 9a and b is reported the comparison from the fluxes obtained by the EC system and the bLS for the two experiments. The coefficient of determination indicates that the bLS slightly overestimates the fluxes in SI-09 (Fig. 9a), while underestimated in SI-11 (Fig. 9b). Dividing fluxes for lower values, less than 10 $\mu g\,m^{-2}\,s^{-1}$, a threshold chosen closer to the averages for EC and bLS fluxes (7.1 and 5.7 $\mu g\,m^{-2}\,s^{-1}$ for EC and bLS in SI-09, respectively; 8.7 and 7.4 $\mu g\,m^{-2}\,s^{-1}$ for EC and bLS in SI-11, respectively), representing the 80% of the data for the two methods and the two trials, different trends can be noticed. In SI-09, there is an overestimation of the fluxes for the bLS method for low flux values (CRM = 1.38), while for high fluxes (>10 $\mu g\,m^{-2}\,s^{-1}$) there is slight under prediction of the EC data by the bLS interpretation (CRM = −0.25). In SI-11 there is a general underestimation for the fluxes lower the imposed threshold (CRM = −5.23) and a general good agreement for higher fluxes (CRM = 0.04). bLS prediction

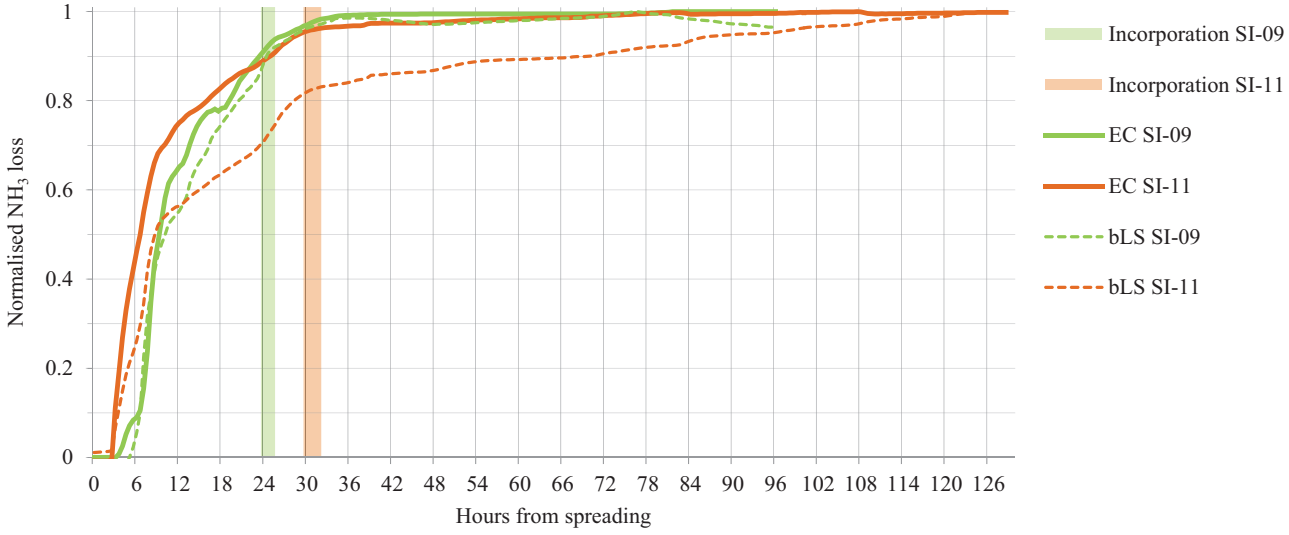

Fig. 8. Cumulate and normalised NH_3 losses measured by the Eddy covariance system (EC) and the backward Lagrangian stochastic model (bLS) during the trials in Landriano 2009 (SI-09) and 2011 (SI-11), over the hours after the spreading.

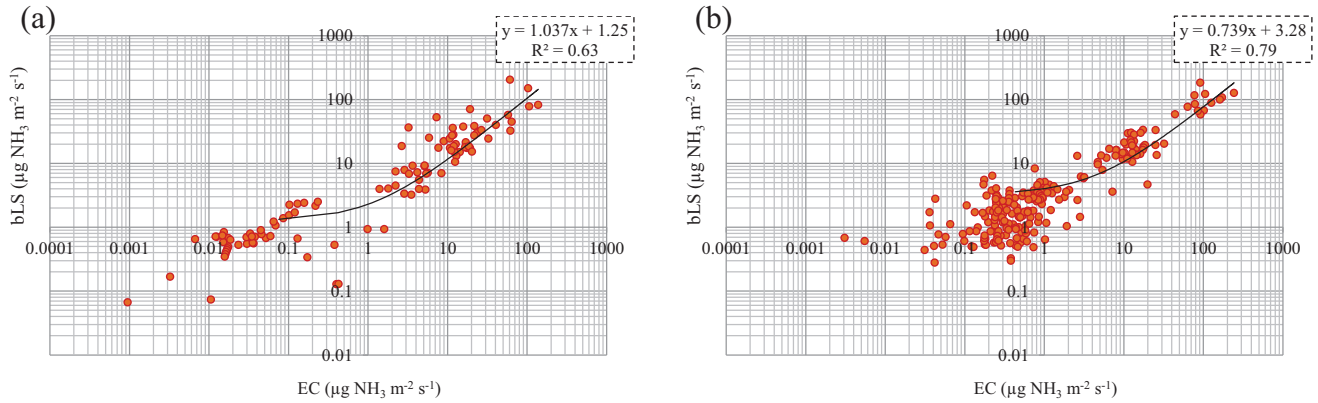

Fig. 9. EC flux measurements compared to concentration-based dispersion modelling estimation (bLS). (a) is the trial in Landriano 2009 (SI-09); (b) the trial in Landriano 2011 (SI-11). Axes are in logarithmic base.

tends to overestimate the fluxes compared to EC, especially during strong stable conditions, while during slight unstable or near neutral atmospheric condition, the trend assume comparable magnitude. The mean absolute error (MAE) from bLS and EC, that express the measures the accuracy for continuous variables, resulted similar for both the experiments (4.3 and 4.7 $\mu g\,m^{-2}\,s^{-1}$ for SI-09 and SI-11, respectively); the RMSE, as well, resulted in the same order of magnitude, 13.2 and 12.0 $\mu g\,m^{-2}\,s^{-1}$ for SI-09 and SI-11, respectively. These results indicate that the bLS estimations and the EC measures have, in both the experiments, small average differences and no large errors. In fact the difference from RMSE and MAE, indicating the magnitude of the variance in each sample, is only 8.5 and 7.6 $\mu g\,m^{-2}\,s^{-1}$. The EF estimated by the bLS model are in the same order of magnitude compared to the EC ones, 24.3% for SI-09 and 33.7% for SI-11; around 15/20% higher than EC measurements. Changing the threshold used to filtered the data with respect to u_* from 0.05 to 0.16 $m\,s^{-1}$, the EF ranged from 24.3 to 28.5% for SI-09 and from 33.7 to 35.9% for SI-11. Since the EF does not change so much in function of the u_* threshold variation, we can assume that a filter of 0.05 it is reasonable for our conditions, as also indicated by Flesch et al. (2014). Moreover, since the turbulence has been lower during SI-11 trial than in SI-09, increasing the u_* threshold generates increasing data exclusion and EF lowering.

The NH_3 volatilisation detected by EC measurements during the two trials followed the typical trend as described by other authors after slurry spreading (Sommer and Hutchings, 2001; Loubet et al., 2010) where the loss rate is usually highest immediately after slurry application and normally falls rapidly. These dynamics could be due to the decrease of concentration of TAN in soil surface due to emission, infiltration or absorption in the soil matrix (Van der Molen et al., 1990; Sommer et al., 2004). Furthermore, the weather pattern plays a fundamental role in the evolution of NH_3 air concentration and fluxes above the treated plots. In fact, in SI-11 trial, when the weather was quite stable during the experiment, the total emission of NH_3 reaches the plateau following a smooth regular pattern, so that in 24 h about 90% of total emission occurred just before the slurry incorporation. Also in SI-09 experiment the same percentage of total emission was reached in the same 24 h after spreading, but with a dissimilar pattern, characterised by a slow rate potentially related to lower temperatures. In this regard, tillage operations after the application of fertilisers, contribute to reducing the emission by incorporating the material into the soil. The timing of tillage is a crucial aspect in the reduction practices. Huijsmans et al. (2003) reported abatement efficiency of 12% if the incorporation of slurry occurs within 24 h, whilst abatement over 90% with an incorporation after 4 h from the spreading. Sadeghpour et al. (2015) reported reduction from 66 to 75% from immediate manure incorporation compared to surface spreading. In the same way Carozzi et al. (2013a) reported abatement of 87% if the slurry incorporation occurs contextually with the spreading, compared to a non-incorporated spreading. In the case reported by the latter Authors, in the non-incorporated trial the 77% of NH_3 volatilised in 24 h from the spreading, highlighting the effect of the timing of the tillage operations.

4. Conclusions

NH_3 volatilisation after slurry spreading has been detected by means EC, whose application has been accurately investigated, facing all issues related to the sticky nature of the gas, the specific setup and all needed corrections (post-processing calibration, high frequency losses ad WPL effect). The statistics at hourly scale demonstrated a good agreement between the calibrated NH_3 concentration values measured by QC-TILDAS and the chemical approach based on ALPHA passive samplers, both in terms of absolute value and the evolution of the process over time. The impact of data treatment on cumulated emissions was evaluated and the filtering process has shown to have a significant influence.

Furthermore, the dynamics of both NH_3 fluxes after slurry spreading and following soil incorporation were similar in the two experimental campaigns, except for slightly difference in the speed of the phenomenon during the first hours, mainly due to different weather patterns.

The comparison from bLS modelling and EC measurements highlight the accordance with the two methods in both the experiments, because of small average differences in the time series and no large errors, demonstrating that the sensors arrangement was suitable to detect all the NH_3 fluxes from the plots. From an agronomic point of view, the slurry incorporation carried after 24 h from the application, proves to be a non-effective abatement strategy, unless this take place in times closer from the spreading itself. This precaution will be able to keep more nitrogen available for cropping growth as it has been demonstrated in recent literature by Carozzi et al. (2013a,b).

Acknowledgements

This study has been founded by the Regional Agency for the Services to Agriculture and Forests (ERSAF) of the Lombardy Region in the ARMOSA project, the Nitroeurope IP founded by the EU's Sixth Framework Programme for Research and Technological Development and the COST Action FP0903.

References

Asman, W.A.H., Sutton, M.A., Schjørring, J.K., 1998. Ammonia: emission, atmospheric transport and deposition. New Phytol. 139, 27–48.

Aubinet, M., Grelle, A., Ibrom, A., Rannik Ü, Moncrieff, J., Foken, T., Kowalski, A.S., Martin, P.H., Berbigier, P., Bernhofer, C., Clement, R., Elbers, J., Granier, A., Grünwald, T., Morgenstern, K., Pilegaard, K., Rebmann, C., Snijders, W., Valentini, R., Vesala, T., 2000. Estimates of the annual net carbon and water exchange of forests: the EUROFLUX methodology. Adv. Ecol. Res. 30, 113–175.

Aubinet, M., Vesala, T., Papale, D., 2012. Eddy Covariance: A Practical Guide to Measurement and Data Analysis. Springer Atmospheric Sciences. Springer-Verlag 438 pp..

Baldocchi, D., 2003. Assessing the Eddy covariance technique for evaluating carbon dioxide exchange rates of ecosystems: past, present and future. Global Change Biol. 9, 479–492.

Bariteau, L., Helmig, D., Fairall, C.W., Hare, J.E., Hueber, J., Lang, E.K., 2010. Determination of oceanic ozone deposition by ship-borne Eddy covariance flux measurements. Atmos. Meas. Tech. 3, 441–455.

Brodeur, J.J., Warland, J.S., Staebler, R.M., Wagner-Riddle, C., 2009. Technical note: laboratory evaluation of a tunable diode laser system for Eddy covariance measurements of ammonia flux. Agric. For. Meteorol. 149, 385–391.

Carozzi, M., Ferrara, R.M., Fumagalli, M., Sanna, M., Chiodini, M.E., Perego, A., Chierichetti, A., Brenna, S., Rana, G., Acutis, M., 2012. Field-scale ammonia emissions from surface spreading of dairy slurry in Po Valley. Ital. J. Agrometeorol. 4, 25–34.

Carozzi, M., Ferrara, R.M., Rana, G., Acutis, M., 2013a. Evaluation of mitigation strategies to reduce ammonia losses from slurry fertilisation on arable lands. Sci. Total Environ. 449, 126–133.

Carozzi, M., Loubet, B., Acutis, M., Rana, G., Ferrara, R.M., 2013b. Inverse dispersion modelling highlights the efficiency of slurry injection to reduce ammonia losses by agriculture in the Po Valley (Italy). Agric. For. Meteorol. 171–172, 306–318.

Clarisse, L., Clerbaux, C., Dentener, F., Hurtmans, D., Coheur, P., 2009. Global ammonia distribution derived from infrared satellite observations. Nat. Geosci. 2, 479–483.

Denmead, O.T., 1983. Micrometeorological methods for measuring gaseous losses of nitrogen in the field. In: Freney, J.R., Simpson, J.R. (Eds.), Gaseous Loss of Nitrogen From Plant–Soil Systems. Kluwer Academic Publisher, Dordrecht, pp. 133–157.

Denmead, O.T., 2008. Approaches to measuring fluxes of methane and nitrous oxide between landscapes and the atmosphere. Plant Soil 309, 5–24.

Detto, M., Verfaillie, J., Anderson, F., Xu, L., Baldocchi, D., 2011. Comparing laser based open- and closed-path gas analyzers to measure methane fluxes using the Eddy covariance method. Agric. For. Meteorol. 151, 1312–1324.

Dragosits, U., Hallsworth, S., Sutton, M.A., 2010. Ammonia Emissions from UK Non-Agricultural Sources in 2008: Contribution to the National Atmospheric Emission Inventory. Edinburgh NERC/Centre for Ecology and Hydrology, pp. 15pp (CEH Project number: C03614).

EEA, 2011. NEC Directive Status Report 2010. Technical Report No. 3/2011. EEA http://www.eea.europa.eu/publications/necdirective-status-report-2010 (accessed 10.12.15).

Eugster, W., Senn, W., 1995. A cospectral correction model for measurement of turbulent NO_2 flux. Boundary-Layer Meteorol. 74, 321–340.

Eugster, W., Zeyer, K., Zeeman, M., Michna, P., Zingg, A., Buchmann, N., Emmenegger, L., 2007. Methodical study of nitrous oxide Eddy covariance measurements using quantum cascade laser spectrometery over a Swiss forest. Biogeosciences 4, 927–939.

Eugster, W., Plüss, P., 2010. A fault-tolerant Eddy covariance system for measuring CH4 fluxes. Agric. For. Meteorol. 150 (6), 841–851.

Famulari, D., Fowler, D., Hargreaves, K., Milford, C., Nemitz, E., Sutton, M., Weston, K., 2004. Measuring Eddy covariance fluxes of ammonia using tunable diode laser absorption spectroscopy. Water Air Soil Pollut. Focus 4 (6), 151–158.

Fehsenfeld, F., 1995. Measurement of chemically reactive gases at ambient concentrations. In: Matson, P.A., Harris, R.C. (Eds.), Biogenic Trace Gases: Measuring Emission from Soil and Water. Blackwell Science, Cambridge, England, pp. 206–258.

Ferrara, R.M., Loubet, B., Di Tommasi, P., Bertolini, T., Magliulo, V., Cellier, P., Eugster, W., Rana, G., 2012. Eddy covariance measurement of ammonia fluxes: comparison of high frequency correction methodologies. Agric. For. Meteorol. 158, 30–42.

Flesch, T.K., McGinn, S.M., Chen, D., Wilson, J.D., Desjardins, R.L., 2014. Data filtering for inverse dispersion emission calculations. Agric. For. Meteorol. 198–199.

Flesch, T.K., Wilson, J.D., Harper, L.A., Crenna, B.P., Sharpe, R.R., 2004. Deducing ground-to-air emissions from observed trace gas concentrations: a field trial. J. Appl. Meteorol. 43 (3), 487–502.

Foken, T., Wichura, B., 1996. Tools for quality assessment of surface-based flux measurements. Agric. For. Meteorol. 78, 83–105.

Foken, T., Aubinet, M., Leuning, R., 2012. The Eddy covariance method. In: Aubinet, M., Vesala, T., Papale, D. (Eds.), Eddy Covariance—A Practical Guide to Measurement and Data Analysis. Springer, Dordrecht, pp. 1–19.

Fratini, G., Ibrom, A., Burba, G.G., Arriga, N., Papale, D., 2012. Relative humidity effects on water vapour fluxes measured with closed-path Eddy-covariance systems with short sampling lines. Agric. For. Meterol. 165, 53–63.

Galloway, J.N., Aber, J.D., Erisman, J.W., Seitzinger, S.P., Howarth, R.W., Cowling, E.B., Cosby, B.J., 2003. The nitrogen cascade. Bioscience 53, 341–356.

Génermont, S., Cellier, P., 1997. A mechanistic model for estimating ammonia volatilization from slurry applied to bare soil. Agric. For. Meteorol. 88, 145–167.

Harper, L.A., 2005. Ammonia: measurement issues. In: Hatfield, J.L., Baker, J.M. (Eds.), Agronomy Mono-graph No. 47, Micrometeorology in Agricultural Systems. ASA-CSSA-SSSA, Madison, WI, pp. 345–380.

Hensen, A., Nemitz, E., Flynn, M.J., Blatter, A., Jones, S.K., Sørensen, L.L., Hensen, B., Pryor, S.C., Jensen, B., Otjes, R.P., Cobussen, J., Loubet, B., Erisman, J.W., Gallagher, M.W., Neftel, A., Sutton, M.A., 2009. Inter-comparison of ammonia fluxes obtained using the Relaxed Eddy Accumulation technique. Biogeosciences 6, 2575–2588.

Hiller, R.V., Zellweger, C., Knohl, A., Eugster, W., 2012. Flux correction for closed-path laser spectrometers without internal water vapor measurements. Atmos. Meas. Tech. Discuss. 5, 351–384. doi:http://dx.doi.org/10.5194/amtd-5-351-2012.

Huijsmans, J.F.M., Hol, J.M.G., Vermeulen, G.D., 2003. Effect of application method, manure characteristics, weather and field conditions on ammonia volatilization from manure applied to arable land. Atmos. Environ. 37, 3669–3680.

Ibrom, A., Dellwik, E., Flyvbjerg, H., Jensen, N.O., Pilegaard, K., 2007. Strong low-pass filtering effects on water vapour flux measurements with closed-path Eddy correlation systems. Agric. For. Meterol. 147, 140–156.

Jarvis, S.C., Pain, B.F., 1990. Ammonia volatilisation from agricultural land. The Fertiliser Society Proceedings. No. 298. The Fertiliser Soc., London, pp. 1–35.

Kaimal, J.C., Finnigan, J.J., 1994. Atmospheric Boundary Layer Flows: Their Structure and Measurement. Oxford University Press 289 pp..

Kolle, O., Rebmann, C., 2007. EddySoft Documentation of a Software Package to Acquire and Process Eddy Covariance Data. Max Planck Institute for Biochemistry, Jena, Germany.

Kormann, R., Meixner, F.X., 2001. An analytical footprint model for nonneutral stratification. Boundary-Layer Meteorol. 99, 207–224.

Lenschow, D.H., Raupach, M.R., 1991. The attenuation of fluctuations in scalar concentration through sampling tubes. J. Geophys. Res. 96 (D8), 15259–15268.

Leuning, R., Moncrieff, J., 1990. Eddy covariance CO_2 flux measurements using open and closed path CO_2 analysers: corrections for analyser water vapour sensitivity and damping of fluctuations in air sampling tubes. Boundary Layer Meteorol. 53, 63–76.

Liebethal, C., Foken, T., 2003. On the significance of the Webb correction to fluxes. Bound-Layer Meteorol. 109, 99–106.

Loubet, B., Cellier, P., Genermont, S., Flura, D., 1999. An evaluation of the wind-tunnel technique for estimating ammonia volatilization from land: part 2. Influence of the tunnel on transfer processes. J. Agric. Eng. Res. 72, 83–92.

Loubet, B., Génermont, S., Ferrara, R.M., Bedos, C., Decuq, C., Personne, E., Fanucci, O., Durand, B., Rana, G., Cellier, P., 2010. An inverse model to estimate ammonia emissions from fields. Eur. J. Soil Sci. 61 (5), 793–805.

Loubet, B., Asman, W.A.H., Theobald, M.R., Hertel, O., Tang, Y.S., Robin, P., Hassouna, M., Dämmgen, U., Genermont, S., Cellier, P., 2009. Ammonia deposition near hot spots: processes, models and monitoring methods. Atmospheric Ammonia. Springer, pp. 205–267.

Mammarella, I., Werle, P., Pihlatie, M., Eugster, W., Haapanala, S., Kiese, R., Markkanen, T., Rannik, Ü., Vesala, T., 2010. A case study of Eddy covariance flux of N_2O measured within forest ecosystems: quality control and flux error analysis. Biogeosciences 7, 427–440.

Massman, 1998. A review of the molecular diffusivities of H_2O, CO_2, CH_4, CO, O_3, SO_2, NH_3, N_2O, NO, and NO_2 in air, O_2 and N_2 near STP. Atmos. Environ. 32 (6), 1111–1127.

Massman, W.J., 2000. A simple method for estimating frequency response corrections for Eddy covariance systems. Agric. For. Meteorol. 104, 185–198.

Massman, W.J., Clement, R., 2004. Uncertainty in Eddy covariance flux estimates resulting from spectral attenuation. In: Lee, X., Massman, W.J., Law, B. (Eds.), Handbook of Micrometeorology. Atmospheric and Oceanographic Sciences Library, Kluwer Academic Publishers, pp. 67–100.

Mauder, M., Cuntz, M., Drüe, C., Graf, A., Rebmann, C., Schmid, H.P., Schmidt, M., Steinbrecher, R., 2013. A strategy for quality and uncertainty assessment of long-term Eddy-covariance measurements. Agric. For. Meteorol. 169, 122–135.

Mauder, M., Foken, T., 2004. Documentation and Instruction Manual of the Eddy Covariance Software Package TK2, vol. 26. Universität Bayreuth, Abt. Mikrometeorologie, Arbeitsergebnisse 44 pp., ISSN 1614-8916.

Misselbrook, T.H., Van Der Weerden, T.J., Pain, B.F., Jarvis, S.C., Chambers, B.J., 2000. Ammonia emission factors for UK agriculture. Atmos. Environ. 34, 871–880.

Moal, J.F., Martinez, J., Guiziou, F., Coste, C.M., 1995. Ammonia volatilization following surface-applied pig and cattle slurry in France. J. Agric. Sci. 125, 245–252.

Moncrieff, J.B., Massheder, J.M., deBruin, H., Elbers, J., Friborg, T., Heusinkveld, B., Kabat, P., Scott, S., Soegaard, H., Verhoef, A., 1997. A system to measure surface fluxes of momentum, sensible heat, water vapour and carbon dioxide. J. Hydrol. 189, 589–611.

Moore, C.J., 1986. Frequency response corrections for Eddy correlation systems. Boundary-Layer Meteorol. 37, 17–35.

Mozurkewich, M., 1993. The dissociation-constant of ammonium-nitrate and its dependence on temperature relative-humidity and particle-size. Atmos. Environ. 27, 261–270.

Nakai, T., van der Molen, M.K., Gash, J.H.C., Kodama, Y., 2006. Correction of sonic anemometer angle of attack errors. Agric. For. Meteorol. 136 (1–2), 19–30.

Neftel, A., Ammann, C., Fischer, C., Spirig, C., Conen, F., Emmenegger, L., Tuzson, B., Wahlen, S., 2010. N_2O exchange over managed grassland: application of a quantum cascade laser spectrometer for micrometeorological flux measurements. Agr. For. Meteorol. 150, 775–785.

Neftel, A., Spirig, C., Ammann, C., 2008. Application and test of a simple tool for operational footprint evaluations. Environ. Pollut. 152 (3), 644–652.
Nelson, D.D., Shorter, J.H., McManus, J.B., Zahniser, M.S., 2002. Sub-part-per-billion detection of nitric oxide in air using a thermoelectrically cooled mid-infrared quantum cascade laser spectrometer. Appl. Phys. B: Laser Opt. 75, 343–350.
Petersen, S.O., Andersen, M.N., 1996. Influence of soil water potential and slurry type on denitrification activity. Soil Biol. Biochem. 28, 977–980.
Reis, S., Pinder, R.W., Zhang, M., Lijie, G., Sutton, M.A., 2009. Reactive nitrogen in atmospheric emission inventories. Atmos. Chem. Phys. 9, 7657–7677.
Sadeghpour, A., Hashemi, M., Weis, S.A., Spargo, J.T., Mehrvarz, S., Herbert, S.J., 2015. Assessing tillage systems for reducing ammonia volatilization from spring-applied slurry manure. Commun. Soil Sci. Plant Anal. 46 (6), 724–735.
Shaw, W.J., Spicer, C.W., Kenny, D.V., 1998. Eddy correlation fluxes of trace gases using a tandem mass spectrometer. Atmos. Environ. 32 (17), 2887–2898.
Sintermann, J., Neftel, A., Ammann, C., Häni, C., Hensen, A., Loubet, B., Flechard, C.R., 2012. Are ammonia emissions from field-applied slurry substantially over-estimated in European emission inventories? Biogeosciences 9, 1 611–1632.
Sintermann, J., Spirig, C., Jordan, A., Kuhn, U., Ammann, C., Neftel, A., 2011. Eddy covariance flux measurements of ammonia by high temperature chemical ionisation mass spectrometry. Atmos. Meas. Tech. 4 (3), 599–616.
Skjøth, C.A., Geels, C., Berge, H., Gyldenkærne, S., Fagerli, H., Ellermann, T., Frohn, L. M., Christensen, J., Hansen, K.M., Hansen, K., Hertel, O., 2011. Spatial and temporal variations in ammonia emissions—a freely accessible model code for Europe. Atmos. Chem. Phys. 11, 5221–5236.
Smeets, C.J.P.P., Holzinger, R., Vigano, I., Goldstein, A.H., Röckmann, T., 2009. Eddy covariance methane measurements at a Ponderosa pine plantation in California. Atmos. Chem. Phys. 9, 8365–8375.
Søgaard, H.T., Sommer, S.G., Hutchings, N.J., Huijsmans, J.F.M., Bussink, D.W., Nicholson, F., 2002. Ammonia volatilization from field-applied animal slurry—the ALFAM model. Atmos. Environ. 36, 3309–3319.
Sommer, S.G., Olesen, J.E., Christensen, B.T., 1991. Effects of temperature, wind speed and air humidity on ammonia volatilization from surface applied cattle slurry. J. Agric. Sci. 117, 91–100.
Sommer, S.G., Hutchings, N.J., 2001. Ammonia emission from field applied manure and its reduction—invited paper. Eur. J. Agron. 15, 1–15.
Sommer, S.G., Hutchings, N.J., Carton, O.T., 2001. Ammonia Losses from Field Applied Animal Manure. Report No. 60, Plant Production. Danish Institute of Agricultural Sciences, Horsens, Denmark.
Sommer, S.G., Schjoerring, J.K., Denmead, O.T., 2004. Ammonia emission from mineral fertilizers and fertilized crops. Adv. Agron. 82, 557–622.
Sutton, M.A., Tang, Y.S., Miners, B., Fowler, D., 2001. A new diffusion denuder system for long-term, regional monitoring of atmospheric ammonia and ammonium. Water, Air and Soil Pollut. Focus 1, 145–156 Part 5/6.
Sutton, M.A., Dragosits, U., Tang, Y.S., Fowler, D., 2000. Ammonia emissions from non-agricultural sources in the UK. Atmos. Environ. 34, 855–869.
Tang, Y.S., Cape, J.N., Sutton, M.A., 2001. Development and types of passive samplers for monitoring atmospheric NO_2 and NH_3 concentrations. Proceedings of the International Symposium on Passive Sampling of Gaseous Pollutants in Ecological Research. TheScientificWorld 1, 513–529.
Van der Molen, J., Beljaars, A.C.M., Chardon, W.J., Jury, W.A., van Faassen, H.G., 1990. Ammonia volatilization from arable land after application of cattle slurry: 2: derivation of a transfer model. Neth. J. Agric. Sci. 38, 239–254.
Van Der Molen, J., Bussink, D.W., Vertregt, N., Van Faassen, H.G., Den Boer, D.J., 1989. mmonia volatilization from arable and grassland soils. In: Hansen, J.A., Henriksen, K. (Eds.), Nitrogen in Organic Wastes Applied on Soils. Academic Press, Londen, pp. 185–201.
von Bobrutzki, K., Braban, C.F., Famulari, D., Jones, S.K., Blackall, T., Smith, T.E.L., Blom, M., Coe, H., Gallagher, M., Ghalaieny, M., McGillen, M.R., Percival, C.J., Whitehead, J.D., Ellis, R., Murphy, J., Mohacsi, A., Junninen, H., Pogany, A., Rantanen, S., Sutton, M.A., Nemitz, E., 2010. Field inter-comparison of eleven atmospheric ammonia measurement techniques. Atmos. Meas. Tech. Discuss. 2, 1783–1835.
Warland, J.S., Dias, G.M., Thurtell, G.W., 2001. A tunable diode laser system for ammonia flux measurements over multiple plot. Environ. Pollut. 114, 215–221.
Webb, E.K., Pearman, G.I., Leuning, R., 1980. Correction of flux measurements for density effects due to heat and water vapour transfer. Q. J. R. Meteorol. Soc. 106, 85–100.
Webb, J., Pain, B., Bittman, S., Morgan, J., 2010. The impacts of manure application methods on emissions of ammonia, nitrous oxide and on crop response—a review. Agric. Ecosyst. Environ. 137, 39–46.
Whitehead, J., Twigg, M., Famulari, D., Nemitz, E., Sutton, M.A., Gallagher, M.W., Fowler, D., 2008. Evaluation of laser absorption spectroscopic techniques for Eddy covariance flux measurements of ammonia. Environ. Sci. Technol. 42, 2041–2046.
Wilczak, J.M., Oncley, S.P., Stage, S.A., 2001. Sonic anemometer tilt correction algorithms. Boundary-Layer Meteorol. 99, 127–150.
Wyers, G.P., Otjes, R.P., Slanina, J., 1993. A continuous-flow denuder for the measurement of ambient concentrations and surface-exchange fluxes of ammonia. Atmos. Environ. 27A, 2085–2090.
Yasuda, Y., Watanabe, T., 2001. Comparative measurements of CO_2 flux over a forest. Boundary-Layer Meteorol. 191–208.